Available online at www.easdprocedia.org
EASD Procedia EURODYN (2020) 2966-2984

EASD Procedia

EURODYN 2020
XI International Conference on Structural Dynamics
M. Papadrakakis, M. Fragiadakis, C. Papadimitriou (eds.)
Athens, Greece, 23–26 November 2020

MITIGATION OF GROUND VIBRATION FROM PILE DRIVING BY CIRCULAR ARRAYS OF RIGID BLOCKS PLACED ON THE GROUND SURFACE

Lars V. Andersen[1], Peter Persson[2], and Andrew T. Peplow[3]

[1] Department of Engineering, Aarhus University
Inge Lehmanns Gade 10, DK-8000 Aarhus C, Denmark
e-mail: lva@eng.au.dk

[2] Department of Construction Sciences, Lund University
P.O. Box 118, SE-221 00 Lund, Sweden
e-mail: peter.persson@construction.lth.se

[3] College of Natural and Health Sciences, Zayed University
P.O. Box 144534, Abu Dhabi, United Arab Emirates
e-mail: andrew.peplow@zu.ac.ae

Keywords: Ground Vibration, Pile Driving, Layered Soil, Insertion Loss, Wave Impedance.

Abstract. *Ground vibration associated with pile driving causes annoyance to inhabitants of the neighbouring environment and may possibly lead to damage on existing structures in the proximity of a construction site. Vibration mitigation near the source can reduce the problem. The paper investigates the effect of circular arrays of blocks, placed on the ground surface around the position at which the pile is driven. A semi-analytical model of a layered soil has been used for the analysis, and the blocks have been modelled as monolithic structures, accounting for the full structure–soil–structure interaction. Two different sites have been studied: a layered soil with three metres of soft sand over a half-space of till, and a five metres deep layer of soft clay overlying a half-space of lime. The block arrays consist of one to three concentric rings with radii 4, 8, and 12 m, respectively. The rings contain 6, 12, and 24 blocks, respectively, and the size of the blocks have been scaled such that each ring has the same total mass. The pile has not been modelled explicitly; instead vertical excitation has been applied in different depts over a circular area corresponding to the cross section of a pile. For the considered cases it has been found that an array of blocks, shaped as a "Stonehenge", may provide significant mitigation of the ground vibration level in a receiver zone placed 20–40 m from the pile. When a load is applied within the soft topsoil layer, the array provides an insertion loss in the order of 5–20 dB, depending on the size of the blocks and the configuration of the arrays. For loads applied deeper in the soil, within the stiffer half-space, the insertion loss is small and may in some situations be negative. However, this must be seen in the context that the transfer mobility in the reference state without the blocks, i.e. the greenfield, is low when the load is applied within the stiff half-space.*

ISSN:2311-9020
Peer-review under responsibility of the Organizing Committee of EURODYN 2020.
doi: 10.47964/1120.9243.20291

1 INTRODUCTION

Environmental vibration from construction activities in urban environments causes annoyance to inhabitants. Long term exposure to noise and vibration may even lead to health problems [1,2], and excessive vibrations can be the cause of damage to structures. Hence, controlling the level of vibrations in the built environment is important.

Several ideas have been proposed for the mitigation of ground vibration from various sources. For rail-traffic-induced vibrations, concepts such as barriers, trenches and soil stiffening [3], [4], or heavy masses placed along the track [5] have been demonstrated to reduce the ground vibration levels in the shielded zones behind the barriers. Also, sheet pile walls in various configurations have been proposed for vibration screening [6–8]. However, installing such barriers will itself cause vibration during the driving of the individual piles.

As an alternative to the continuous barriers, wave impedance blocks (WIBs) placed on the ground surface or embedded within the soil can be used for the reduction of ground vibration [9–11]. Masoumi et al. [12] reported an experimental validation of the mitigation provided by such systems. WIBs – or another change in geometry or material – can be placed in a periodic array. Following the original idea of Mead [13], wave propagation in certain frequency bands can thereby be reduced significantly, theoretically leading to the presence of stop bands (or band gaps) with no propagation of energy. In this context, Persson et al. [14] suggested the reshaping of a landscape into an array of hills and/or valleys, while Andersen [15] analysed the effect of linear arrays of embedded WIBs using a two-dimensional model. The study was later extended to finite arrays in three-dimensions [16–18]. Also, simplified models were proposed for fast, preliminary analysis of WIB arrays placed on the ground surface [19,20].

Returning to the particular vibration problem related to installation of piles, a thorough study on the wave propagation via the soil and into buildings, including the effect on the structure and the occupants, was conducted by Athanasopoulos and Pelekis [21]. More recently, the vibratory sheet pile driving was studied by Deckner et al. [22–24]. The vibrations transmitted via the ground carry most of the energy in the frequency range relevant for whole-body vibrations, i.e. in the range 1–80 Hz. Further, buildings (or structural elements such as floors or walls) may resonate at the excitation frequencies involved in vibratory or impact pile driving [21].

A means of mitigating the ground vibrations from pile driving is therefore beneficial but demands that it can be realized at a low cost and without causing additional vibration. The use of WIBs placed on top of the ground could provide an efficient solution, by using a system of large construction waste-bags or other types of containers that can be filled with locally available material (excavated soil, recycled concrete, etc.), the work involved in establishing the vibration mitigation system would be minimal. Based on this idea, the authors previously proposed the introduction of a circular array of WIBs placed around a vibration source acting on the ground surface [25]. Different configurations of the array were tested, using a semi-analytical model. The main findings were that the WIB arrays provided an insertion loss (IL) of up to 20 dB in the vertical ground vibration levels, defined as the mean value in the zone 20–40 m away from the source. The effect was particularly pronounced at frequencies just above cut-on for wave propagation in soft topsoil, where the vibration levels peaked in the reference case without the WIBs. Also, an array with a configuration mimicking that of Stonehenge (with large blocks in the centre ring and gradually smaller blocks in the surrounding rings) was in many situations found to be more effective than arrays with block of equal size in all rings.

However, whereas Andersen et al. [25] concluded that the circular WIB arrays may be efficient for ground vibration mitigation related to surface sources, no analyses of buried sources or pile driving were performed. This paper, on the other hand, has focus on the IL related to vibrations generated by excitation at various depths below the ground surface. The frequency

range 0–80 Hz has been considered, as this is relevant for whole-body vibration and for the first eigenmodes of typical building elements and resonance in soil layers. To allow a direct comparison with the earlier findings, it has been chosen to use the same soil stratifications, i.e. 3 m of soft sand over a till half-space (Case 1), and 5 m of soft clay over a lime half-space (Case 2). However, compared to [25], only the "Stonehenge" configuration of the WIB array has been analysed in the paper. Ideally, to study the vibration from pile driving, a numerical model should account for the nonlinear response of the pile–soil system as proposed, for example, by Rooz et al. [26]. However, for a conceptual feasibility study of the suggested mitigation strategy, we propose the use of a simplified methodology. Hence, a linear viscoelastic model is used for the ground, and the pile is not modelled explicitly. Instead, vibration sources at various depths in the ground are considered. During the driving process, a pile will transfer energy to the soil, partly along the shaft, and partly at the tip. The proposed model allows a quantification of the IL that can be achieved for the contributions at each separate depth, but because of the simplified modelling approach it cannot be used for the assessment of the overall vibration levels.

The remaining parts of the paper are structured as follows. First, Section 2 describes the computational model. Then, Sections 3 and 4 provide the results and a discussion of the IL achieved in Cases 1 and 2, respectively. Finally, the main conclusions and suggestions for further research are given in Section 5.

2 SEMI-ANALYTICAL MODEL FOR THE SOIL AND RIGID BLOCKS

2.1 Transfer-matrix method for a layered ground with embedded sources

The analyses concern the vibration propagation into the far field, and in the case of man-made vibration due to pile driving, the cyclic shear strain magnitudes are small enough that a linear viscoelastic behaviour of the soil can be assumed. With wavelengths much longer than the characteristic grain size, a solid continuum model can be applied. The half-space $x_3 \leq 0$ is considered, assuming the ground surface and any internal interfaces to be horizontal. Given the linearity and horizontal invariance of the problem, the displacement in direction i at any point (x_1, x_2, x_3) and time t can be found as

$$u_i(x_1, x_2, x_3, t) = \int_{-\infty}^{0}\int_{-\infty}^{\infty}\int_{-\infty}^{\infty}\int_{-\infty}^{t} g_{ij}(x_1 - y_1, x_2 - y_2, x_3, y_3, t - \tau) \times p_j(y_1, y_2, y_3, \tau)\, \mathrm{d}\tau\, \mathrm{d}y_1\, \mathrm{d}y_2\, \mathrm{d}y_3, \qquad x_3 \leq 0\,, \quad (1)$$

where $g_{ij}(x_1 - y_1, x_2 - y_2, x_3, y_3, t - \tau)$ is the Green's function for the half-space, and $p_j(y_1, y_2, y_3, \tau)$ is the load applied at the position (y_1, y_2, y_3) and time τ.

The Green's function in the time–space domain cannot be found in closed form for a layered half-space. Instead, Eq. (1) is Fourier transformed into the frequency–horizontal wavenumber domain, arriving at the equation

$$\bar{U}_i(k_1, k_2, x_3, \omega) = \sum_{n=1}^{N_\mathrm{P}} \bar{G}_{ij}(k_1, k_2, x_3, y_{3n}, \omega)\, \bar{P}_j(k_1, k_2, y_{3n}, \omega). \quad (2)$$

$\bar{U}_i(k_1, k_2, x_3, \omega)$ is the triple Fourier transform of $u_i(x_1, x_2, x_3, t)$, while $\bar{P}_j(k_1, k_2, y_{3n}, \omega)$ is the triple Fourier transform of $p_j(y_1, y_2, y_3, \tau)$, and $\bar{G}_{ij}(k_1, k_2, x_3, y_3, \omega)$ is the triple Fourier transform of $g_{ij}(x_1 - y_1, x_2 - y_2, x_3, y_3, t - \tau)$. A discretization has been made in order to evaluate the contributions from a finite set of loads applied at the depths y_{3n}, $n = 1,2, \ldots, N_\mathrm{P}$. For each discrete depth that is not coinciding with an interface between two soil layers or the ground surface, an additional interface must be introduced in the model.

The material properties of each soil layer are defined in terms of the shear modulus G, Poisson's ratio ν, the mass density ρ, and the loss factor η. Thus, rate-independent hysteretic material damping is assumed, leading to a complex-valued dynamic stiffness of the soil. Next, for any combination of the source and receiver depths, x_3 and y_{3n}, the horizontal wavenumbers (k_1, k_2), and the angular frequency ω, an analytical solution for $\bar{G}_{ij}(k_1, k_2, x_3, y_{3n}, \omega)$ can be found by the layer transfer matrix-method proposed by Thomson [27] and Haskell [28]. The efficient implementation of Andersen and Clausen [29] has been used for the present analysis, augmented by the stabilization method proposed by Wang [30]. This allows a fast calculation of the response without necessitating a discretization over depth by the thin-layer method.

Once, $\bar{G}_{ij}(k_1, k_2, x_3, y_{3n}, \omega)$ and $\bar{P}_j(k_1, k_2, y_{3n}, \omega)$ have been evaluated for a given angular frequency, a double inverse Fourier transformation can be carried out with respect to k_1 and k_2 in order to obtain the solution in the frequency–space domain, $G_{ij}(x_1 - y_1, x_2 - y_2, x_3, y_3, \omega)$. In the present work, the load is assumed to be distributed uniformly over a circular horizontal area with a radius of $r_\mathrm{P} = 0.25$ m, corresponding to the cross section of the pile at a given depth. Hence, the load is axisymmetric. The same property applies to the Green's function, given the horizontal invariance of the stratification. This allows the double inverse Fourier transformation to be carried out in a semi-discrete manner with analytic transformation over the azimuth direction and discrete Fourier transformation in the radial direction. A discretization into 10 000 wavenumbers along the radial direction has been used, focussing on the range relevant to waves propagating in the layered medium, and Simpson integration has been applied for increased accuracy [29]. Since the frequency domain is considered in the present analyses, further inverse Fourier transformation into the time domain should not be carried out.

2.2 Rigid blocks interacting dynamically with the soil

An array with N_B rigid blocks is considered. The blocks are placed on the ground surface, and the dynamic soil–structure interaction (SSI) is modelled, discretizing the interface between each block and the soil into N_ssi points. The blocks have a rectangular footprint of 1 m × 2 m for the inner ring of the circular array, and smaller for the other rings. This footprint is discretized into 6 × 12 points. Around each of the SSI points, the traction is distributed uniformly over a circular area with the radius $r_\mathrm{ssi} = r_\mathrm{P} = 0.25$ m. Hence, the circular loaded areas have a small overlap, and a total of $N_\mathrm{SSI} = N_\mathrm{ssi} N_\mathrm{B} = 72 N_\mathrm{B}$ SSI points are present.

Unit loads will be applied, in turn, at a set of N_P source points. This adds N_P degrees of freedom (d.o.f.) to the problem. Thus, the model has $3N_\mathrm{P} + 3N_\mathrm{SSI}$ displacement d.o.f., leading to a global flexibility matrix $\mathbf{C}_\mathrm{SSI}(\omega)$, the elements of which are defined by the Green's function $G_{ij}(x_1 - y_1, x_2 - y_2, x_3, y_{3n}, \omega)$ that relates $U_i(x_1, x_2, x_3, y_{3n}, \omega_n)$ to $P_j(y_1, y_2, x_3, y_{3n}, \omega_n)$.

Since each rigid block has six d.o.f., $6N_B$ rigid-body modes exist for the array, in addition to the $3N_\mathrm{P}$ degrees of freedom associated with the source points. The relationship between the $3N_\mathrm{P} + 3N_\mathrm{SSI}$ d.o.f. and the $3N_\mathrm{P} + 6N_\mathrm{B}$ rigid-body modes is defined in terms of the matrix $\mathbf{U}_0$, and the dynamic stiffness matrix $\mathbf{D}_\mathrm{SSI}(\omega)$ for the reduced model can be found as

$$\mathbf{D}_\mathrm{SSI}(\omega) = \mathbf{U}_0^T \left(\mathbf{C}_\mathrm{SSI}(\omega)\right)^{-1} \mathbf{U}_0, \tag{3}$$

which has the dimensions $\left((3N_\mathrm{P} + 6N_\mathrm{B}) \times (3N_\mathrm{P} + 6N_\mathrm{B})\right)$. The displacement response at a set of receiver and observation points can finally be determined by postprocessing. Here, the donut-shaped area with inner radius 20 m and outer radius 40 m, centred at the load, is considered, using a pattern of nearly regular triangle with 0.5 m between the receiver points in the radial direction and approximately 1 m distance in the azimuthal direction. This provides 14 520 points in the receiver zone. Following the same discretization strategy, 4 921 observation points are present on the ground surface within the circular area inside the donut-shaped receiver zone.

2.3 Configurations of the rigid blocks and the loads

In the previous work by the authors [25], different configurations of circular WIB arrays were considered. Here, we shall only consider the so-called "Stonehenge" configuration. The WIBs are placed on the surface of the ground, forming one, two or three concentric rings. The radii are 4 m, 8 m, and 12 m, respectively, and the loads are applied at the centre of the rings at some depth below the ground surface. The reference point for each of the rigid blocks is placed at the centre of the rectangular base, i.e. in the centre of the SSI interface for each block. The number of blocks in Rings 1, 2 and 3 is 6, 12 and 24, respectively, as shown in Figure 1a.

The inner ring (Ring 1) serves as the reference in terms of block dimensions. As mentioned, the blocks in this ring have a rectangular footprint of the dimensions 1 m × 2 m. The shorter side length is in the radial direction, while the longer side length is tangential to the ring. Three different block heights are considered: 1 m, 2 m, and 3 m. The WIBs in Rings 2 and 3 are scaled uniformly in all directions, thus keeping the aspect ratio. The scaling factors $0.5^{1/3}$ and $0.5^{2/3}$ are used for the blocks in Rings 2 and 3, respectively, such that the total volume of the blocks in each ring will be the same. For example, with a height of 2 m and a mass density of 2 000 kg/m^3, corresponding to dense soil or granulated concrete, the mass of the blocks in Ring 1 is 4 000 kg each, while the individual blocks in Rings 2 and 3 have masses of 2 000 kg and 1 000 kg, respectively. Again, it is noted that such blocks could, for example, by realized by filling some type of containers with material that is already present at the construction site.

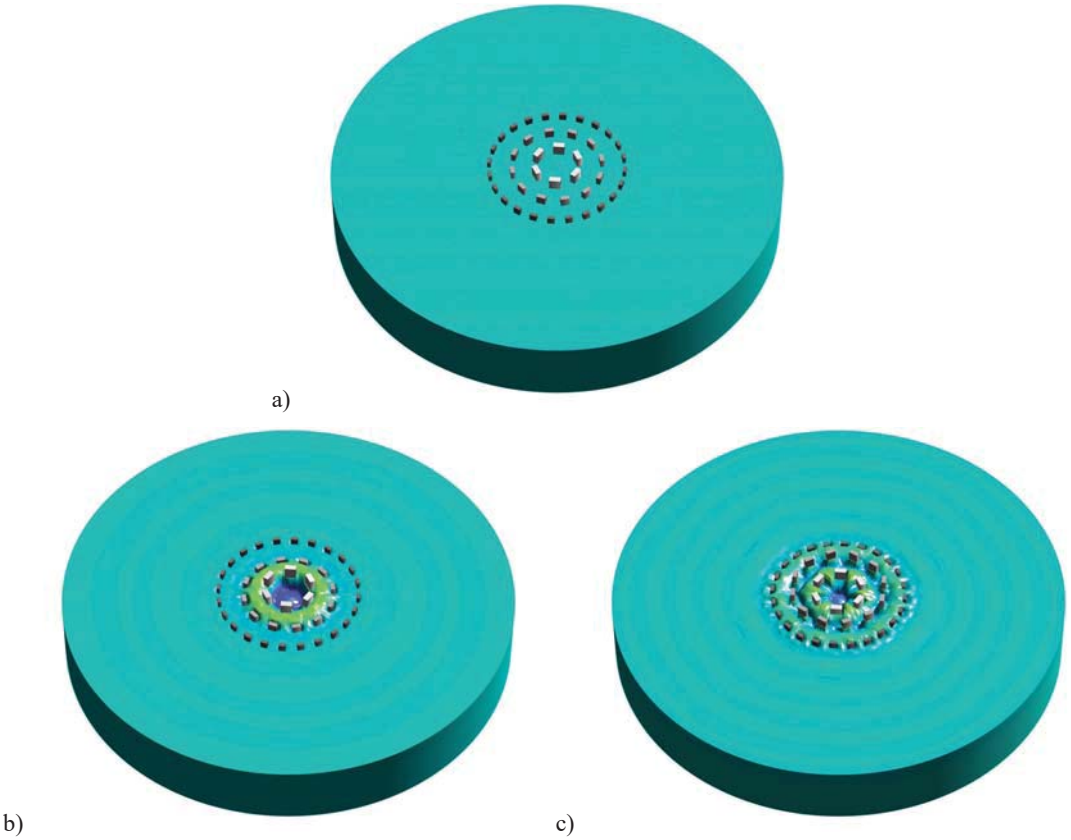

Figure 1: Model and example results: a) Configuration of the rigid blocks (WIBs) in the "Stonehenge" with three rings; b) ground vibration at 25 Hz; c) ground vibration at 30 Hz. The radii of the rings are 4 m, 8 m and 12 m, respectively, and the radius of the model is 40 m. The load is placed 2 m below the ground surface and applied vertically, uniformly distributed over a circular area with a radius of 0.25 m.

Figure 1b shows the ground displacement at 25 Hz due to a load applied 2 m below the ground surface and with three rings of WIBs placed in a "Stonehenge". The centre block height is 2 m, and the soil consists of 3 m of soft dry sand underlain by a till half-space (see Section 3, Table 1, for soil properties). Figure 1c shows the similar results at 30 Hz. At 25 Hz the displacement response is confined within the second ring, whereas large vibrations reach the third ring at 30 Hz. However, a clear effect is seen in the figure for both frequencies.

2.4 Insertion loss and transmission loss in the receiver zone

At any frequency, the vibration level in the receiver zone is influenced by 1) the source magnitude, geometry and position; 2) the transmission through the soil and any structures present within the close environment; and 3) the effect of the WIB array. A detailed discussion of the source is beyond the scope of the paper. However, assuming linear behaviour, the response scales linearly with the source magnitude. Further, as already mentioned, the load is applied uniformly on a circular area that could represent the cross section of a pile at a given depth.

Regarding the transmission of vibration through the soil, we assume that no obstacles or structures are present, except for the WIBs. The reference level (RL) for vibrations in the donut-shaped receiver zone is therefore taken as the level observed in the greenfield. In decibels, the RL for any point on the ground surface ($x_1, x_2, x_3 = 0$) and angular frequency ω is defined as

$$\mathrm{RL}_i^n(x_1, x_2, \omega) = 20\log_{10}\left(\left|U_i^{0n}(x_1, x_2, \omega)\right|\right) - 20\log_{10}(U_{\mathrm{ref}}). \tag{2}$$

Here $U_i^{0n}(x_1, x_2, \omega)$ is the ground surface displacement amplitude for a unit-magnitude (1 N) vertical distributed load applied around a source point at depth y_{3n}, and $U_{\mathrm{ref}} = 100$ pm. Only the vertical vibrations are considered. Thus, only $RL_3(x_1, x_2, \omega)$ is evaluated for the points within the receiver zone. Since a unit-magnitude load is applied, the RL may be regarded as a transfer mobility in dB for the layered ground.

The effect of a WIB array can be quantified in terms of an IL, defined as the difference in dB between the observed vibration levels before and after introducing the WIBs. Hence, a positive insertion loss implies a reduction in vibration level. For displacement component i, WIB configuration j, and pile (load) depth n, the IL is given as

$$\mathrm{IL}_i^{nj}(x_1, x_2, \omega) = 20\log_{10}\left(\left|U_i^{0n}(x_1, x_2, \omega)\right|\right) - 20\log_{10}\left(\left|U_i^{nj}(x_1, x_2, \omega)\right|\right), \tag{3}$$

where $U_i^{nj}(x_1, x_2, \omega)$ is the surface displacement amplitude obtained by applying the unit-magnitude load, i.e. the transfer mobility, after insertion of the WIB array. Again, only vertical vibration is considered, i.e. only $\mathrm{IL}_3^{nj}(x_1, x_2, \omega)$ is evaluated at the 3 780 receiver points.

To assess the importance of mitigation of ground vibration at a given frequency, it is necessary to study the RL and IL in combination. If the RL is high and the IL is low in a range of frequencies relevant to the generation of vibrations at the source, the received vibration level will be high. On the other hand, if the RL is low, a small (or even negative) IL can be tolerated, especially if the source level is also anticipated to be relatively low. This will form the basis for the discussion of the results presented in the following sections. As outlined in the introduction, two cases will be considered:

- Case 1: 3 m soft sand over a till half-space
- Case 2: 5 m soft clay over a lime half-space.

As a single measure of the RL and IL for different WIB arrays, the mean values of the RL and IL within the receiver zone will be used. The variation within the receiver zone is visualized by further calculating the 10% and 90% quantiles of the RL and IL.

3 CASE 1: 3 METRES OF SOFT DRY SAND OVER A HALF-SPACE OF TILL

The material properties for the soft sand layer and the underlying till half-space are given in Table 1. To examine the effect of the block height, three subcases are considered:

- Case 1.1: 1 m high blocks in Ring 1, and with either one, two or three rings
- Case 1.2: 2 m high blocks in Ring 1, and with either one, two or three rings
- Case 1.3: 3 m high blocks in Ring 1, and with either one, two or three rings.

It is noted that the blocks in Rings 2 and 3 will be smaller than those in Ring 1, as explained in Subsection 2.3 and shown in Figure 1a.

The blocks act as monolithic structures. The mass is proportional to the height, whereas the stiffness related to the soil–structure interaction is invariant to the block height. Hence, WIBs with different heights will resonate at different frequencies. This is even more pronounced for the pitch and rolling modes (or rocking) of the blocks, since a part of the rotational inertia scales with the cube of the height. Further, since the blocks in the Rings 1, 2 and 3 are not of the same size, the resonance frequencies will differ. The values are provided in Table 2, based on the static stiffness of the soil and the inertia of the blocks. It has been judged that the vertical vibration levels in the receiver zone are mainly influenced by the vertical motion (heave) of the blocks, their horizontal sliding, and their pitch rotation around the axis tangential to the perimeter of the ring. Hence, only the frequencies related to resonance in these modes are given.

An important observation can be made regarding the resonance frequencies in Table 2: they all lie in the frequency range 0–80 Hz, which is relevant to whole-body vibrations and building vibration. Further, this is the frequency range where most of the energy will be present in the excitation due to pile driving, and it may be expected that guided waves may be generated in the soft sand layer within this frequency range. The ratios between the resonance frequencies for the blocks and the cut-on frequencies for the layer waves can be expected to have an influence on the IL. Obviously, the mass of the WIBs will itself be important, since a heavier mass requires more energy to be moved.

The transfer mobility of the stratified soil, quantified in terms of the RL, depends strongly on whether the load is applied within the top layer of soft soil or within the underlying and much stiffer half-space. However, it has been found that the response is only marginally influenced by the relative depth of the load within the layer. Hence, to avoid an over-excessive number of figures, only two source points ($n = 2, 8$) will be considered, that is: $y_{3\,2} = -2$ m (which is inside the topsoil layer) and $y_{3\,8} = -8$ m (which is within the underlying half-space).

Soil layer (from top)	Shear modulus G [MPa]	Poisson's ratio ν [-]	Mass density ρ [kg/m^3]	Loss factor η [%]	Thickness h [m]
Sand, *soft, dry*	35.72	0.3330	1 553	4.50	3.0
Till (half-space)	500.0	0.3500	2 100	2.00	∞

Table 1: Soil properties for Case 1.

	Blocks in Ring 1			Blocks in Ring 2			Blocks in Ring 3		
	Heave	Sliding	Pitch	Heave	Sliding	Pitch	Heave	Sliding	Pitch
Case 1.1	34.8	30.0	24.6	42.4	36.9	31.7	52.6	46.0	37.2
Case 1.2	24.6	21.2	9.41	30.0	26.1	12.3	37.2	32.5	14.3
Case 1.3	20.1	17.3	5.21	24.5	21.3	6.84	30.3	26.6	7.90

Table 2: Resonance frequencies (in Hz) of the blocks in Case 1.

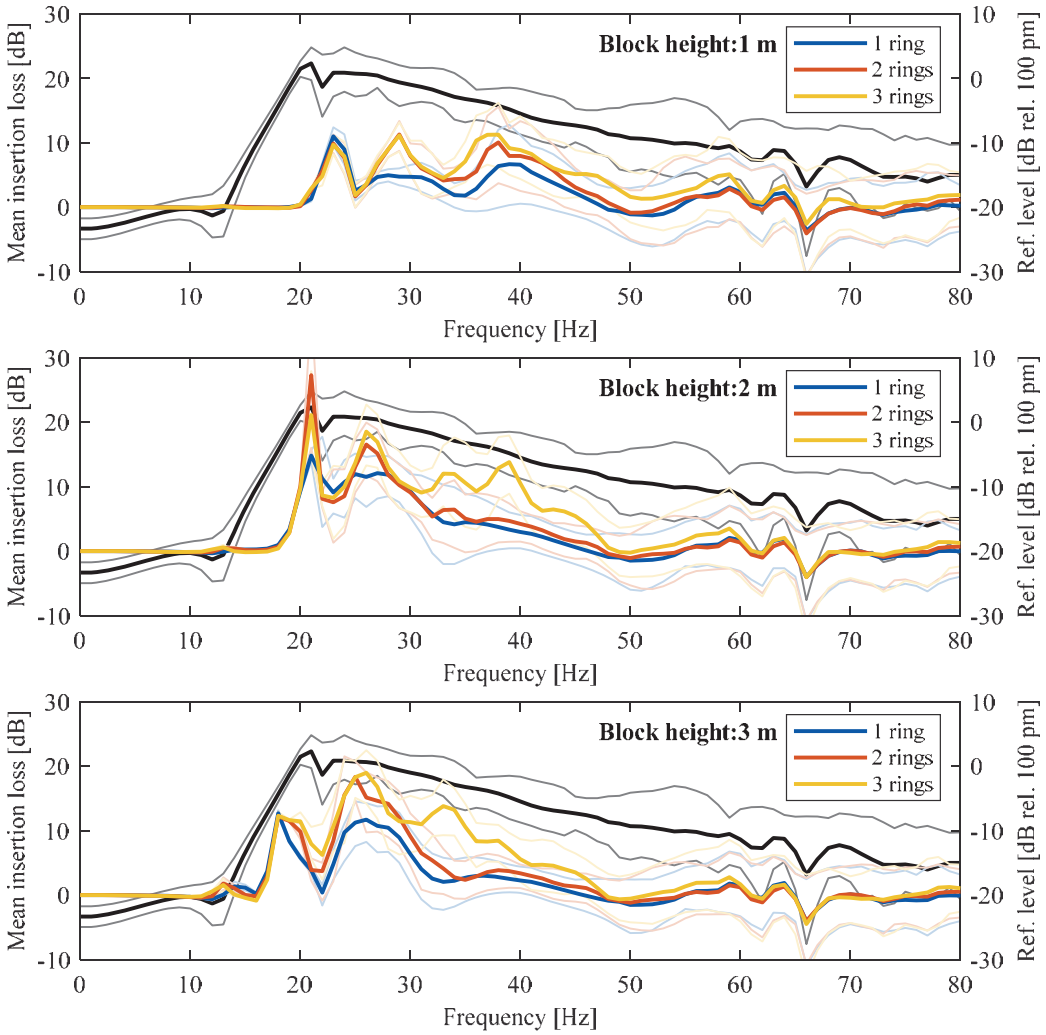

Figure 2: Mean ILs for the ground vibration within the donut-shaped surface area placed 20–40 m away from the centre of the load: Cases 1.1, 1.2, and 1.3, with the load acting 2 m below the ground. The black lines show the reference level of vibrations and the thin lines show the 10% and 90% quantiles of the respective quantities.

For the load depth of 2 m, Figure 2 shows the mean and the 10% and 90% quantiles of the RL (black lines) in Case 1. Further, the figure shows the mean and quantile values for the IL achieved with 1, 2 or 3 rings in the "Stonehenge" in Cases 1.1 (1 m high blocks in Ring 1), 1.2 (2 m high blocks in Ring 1), and 1.3 (3 m high blocks in Ring 1). For frequencies below 12.5 Hz, the RL is relatively small, about –22 dB rel. 100 pm. Then, within the interval 12.5–20 Hz, the RL increases to about 0 dB, indicating the presence of a cut-on frequency for wave propagation in the top layer at approximately 12.5 Hz. The shear wave velocity in the soft sand is about 150 m/s, which leads to a wavelength of 12 m at this frequency. Hence, the layer thickness matches with one quarter of a wavelength, which leads to resonance. From 20 Hz and up to 50 Hz, the RL decreases almost monotonously. This can be attributed to material dissipation and less constructive interference of waves. Beyond 50 Hz, where the shear wavelength becomes smaller than the layer thickness, the response varies differently.

For the various configurations of the WIB arrays, the IL peaks somewhere in the frequency range 18–38 Hz, with the exact position of the peak being dependent on the block height and

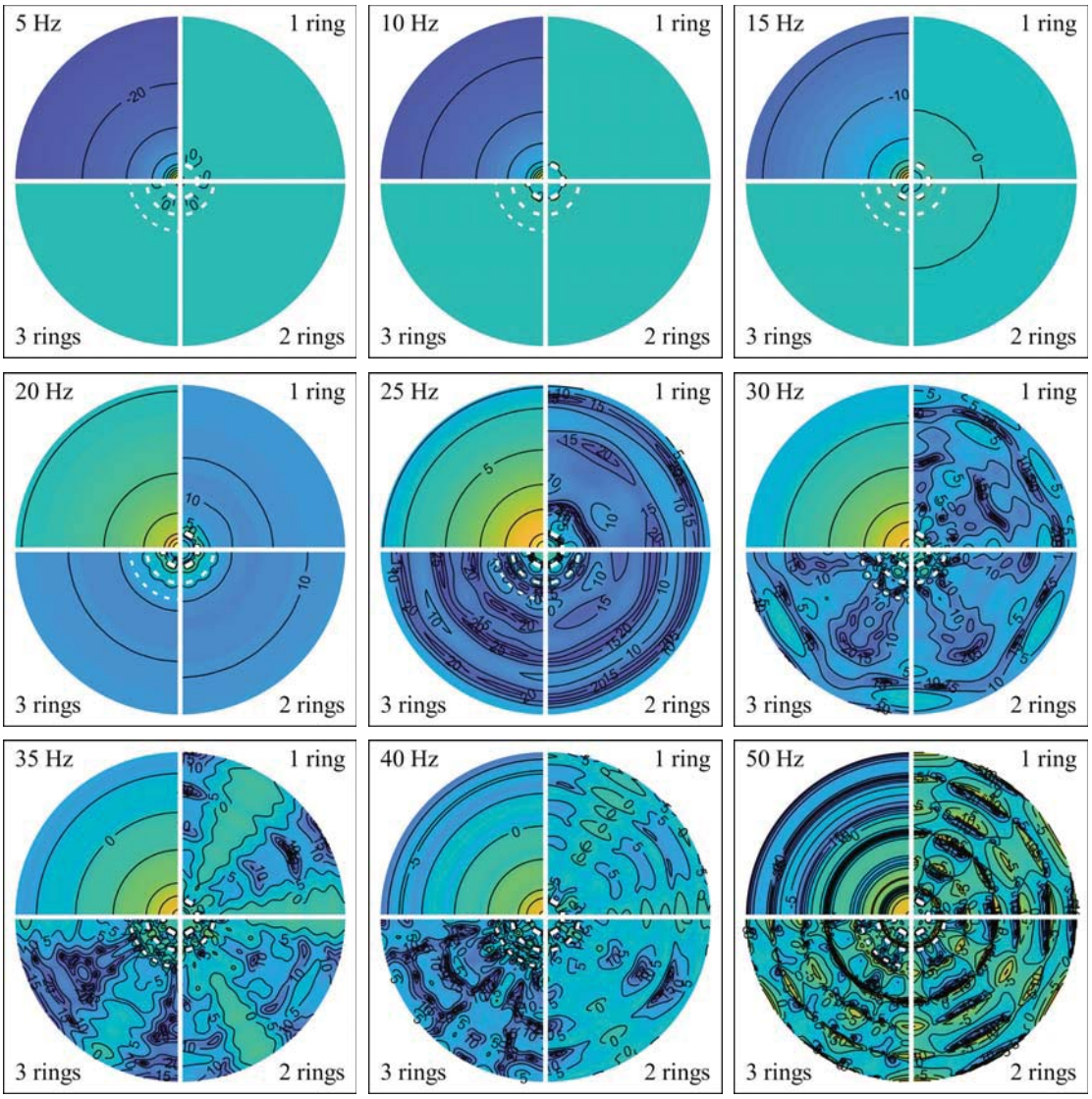

Figure 3: Contours of the reference vibration levels and ILs (in dB) for Case 1.2 with 1, 2, or 3 rings. The centre blocks are 2 m high and the vertical load is applied 2 m below the ground surface. Pale yellow/dark blue shades represent unfavourable/favourable values, respectively.

number of rings. In Case 1.1, with all three rings present, the IL is around 5–10 dB in the range 22–60 Hz, with some tips and dips. This configuration is more effective (providing higher IL than the other configurations) in the frequency range 35–80 Hz. The 1 m high blocks even provide a larger IL than the 2 or 3 m high blocks in the frequency range 45–60 Hz. However, a larger IL is obtained from 17 to 35 Hz in Cases 1.2 and 1.3. In most of the tested scenarios, the IL increases with the number of rings. As an exception, Case 1.2 is particularly effective around 21 Hz when only two rings are present. Also, in Cases 1.1 and 1.2, one ring of WIBs provides slightly higher IL than two or three rings around 23 Hz. Figure 3 shows the RL (top left quadrants of the subplots) and IL (remaining quadrants of the subplots) on the ground surface at nine selected frequencies for Case 1.2. The figure clearly shows that the array has limited effect for frequencies below 15–20 Hz. For frequencies higher than 25 Hz, the IL is subject to large variation within the receiver zone, which can also be seen from the quantile lines in Figure 2.

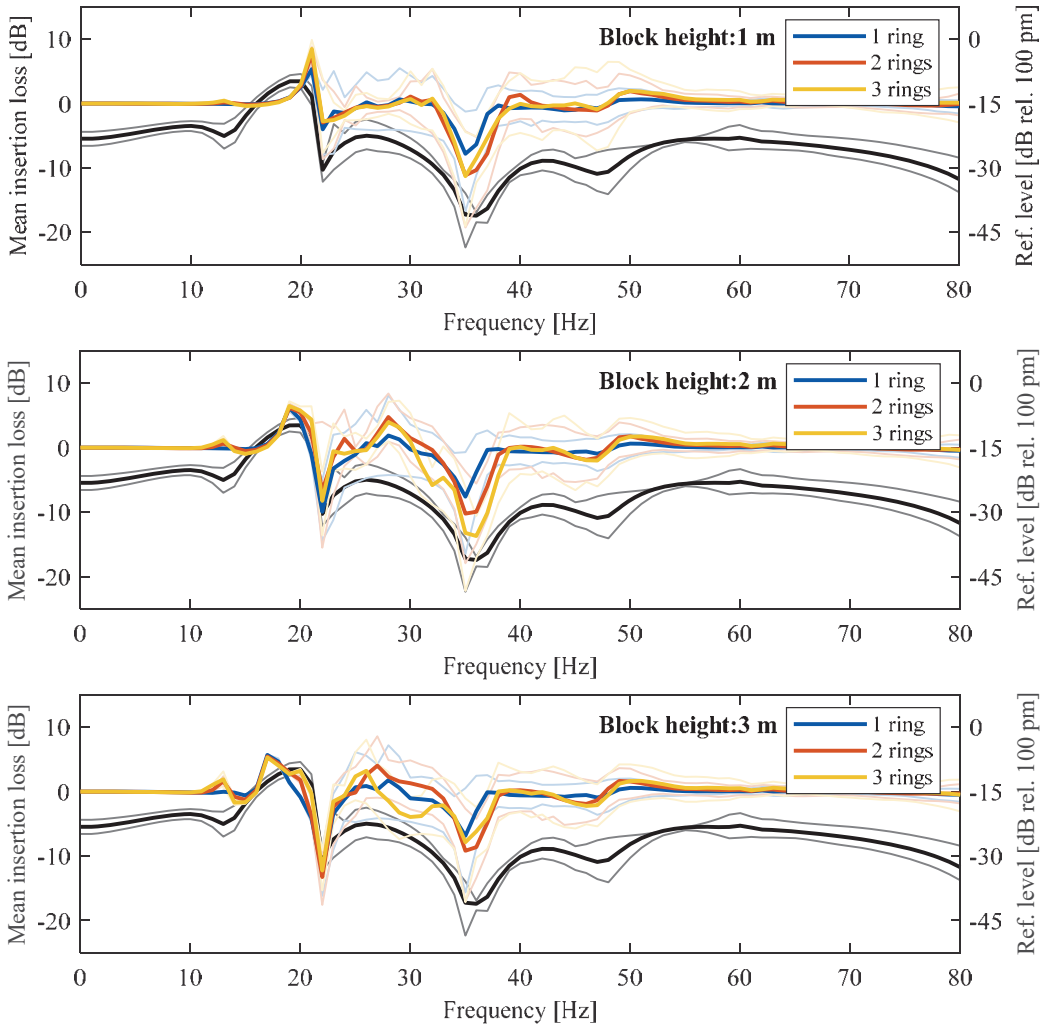

Figure 4: Mean ILs for the ground vibration within the donut-shaped surface area placed 20–40 m away from the centre of the load: Cases 1.1, 1.2, and 1.3 with the load acting 8 m below the ground. The black lines show the reference level of vibrations and the thin lines show the 10% and 90% quantiles of the respective quantities.

Figure 4 shows the mean and quantile values of the RL and IL in the receiver zone for Case 1 with the load applied at $y_{3\,8} = -8$ m. As an example of the local variations of the RL and IL within the receiver zone for this load depth, Figure 5 shows the results for Case 1.2, i.e. with a block height of 2 m in Ring 1. The WIB arrays have limited effect for frequencies below 15–20 Hz, similarly to the case with the load depth of 2 m. However, for the frequency range 12–55 Hz, the IL varies significantly and is, in some cases, negative, down to about –15 dB. The negative IL associated with the 2 and 3 m high blocks is more pronounced around 22 Hz, whereas the 1 and 2 m high blocks lead to lower IL around 35 Hz. However, with reference to Figure 2, this is where the higher IL is obtained when the load is applied at $y_{3\,2} = -2$ m.

Hence, a given configuration of the WIB array may provide a high IL in some frequency range when the load is applied at one depth, but it may be ineffective – or even amplify the ground vibration – in the same frequency range when the load is applied at another depth. A comparison of Figures 2 and 4 shows that the RL is about 20–30 dB lower when the load is applied at 8 m depth, compared to the load applied 2 m below the ground surface. This indicates

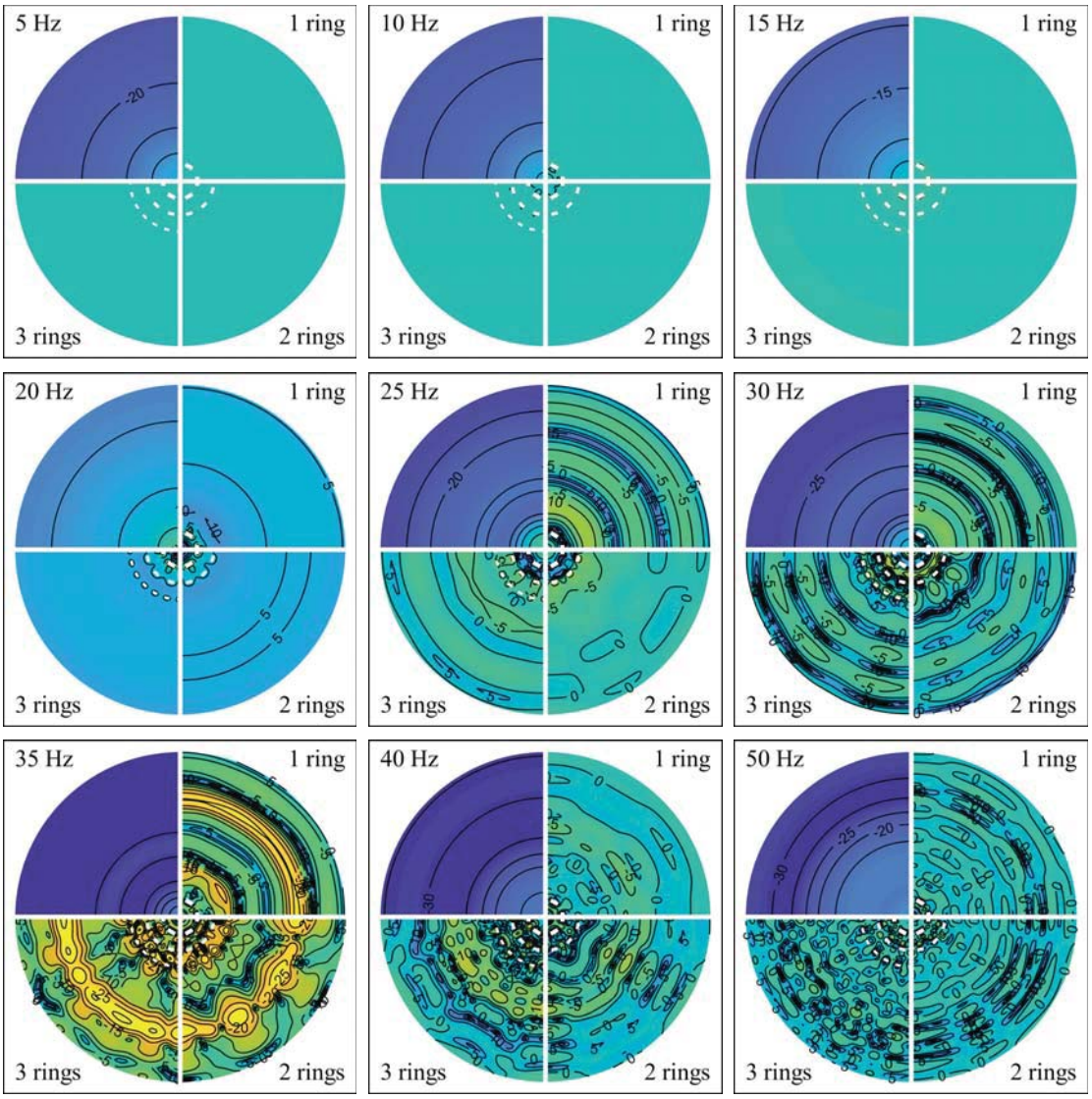

Figure 5: Contours of the reference vibration levels and ILs (in dB) for Case 1.2 with 1, 2, or 3 rings. The centre blocks are 2 m high and the vertical load is applied 8 m below the ground surface. Pale yellow/dark blue shades represent unfavourable/favourable values, respectively.

that the vibrations will not be trapped within, and guided by, the soft topsoil layer. In any case, the resulting vibration level in the receiver zone can be found as the RL minus the IL. Since the mean value of $\mathrm{RL}_3^8 - \mathrm{IL}_3^{8j}$ is well below zero for all considered frequencies, the poor performance of the WIB arrays for the deeper source has limited consequences for the overall quality of the mitigation technique. Instead, the WIB arrays imply a significant reduction of the vibration level when the load is applied within the soft top layer, exemplified by $y_{3\,2} = -2$ m. At these frequencies, the RL is around 0 dB. With reference to Table 2 and Figure 2, the larger values of IL_3^{2j} are present within the frequency range where the WIBs may resonate. Hence, depending on the soil stiffness, the WIBs can be designed to resonate in the frequency range for which a high IL is required. The size of the blocks and their the height relative to the footprint are design variables. To make adjustments on site, the height can be changed, e.g., by filling more soil or granulated concrete into containers, such as large construction waste-bags.

4 CASE 2: 5 METRES OF SOFT CLAY OVER A HALF-SPACE OF LIME

The site considered in Case 2 has a 5 m layer of soft wet clay underlain by a lime half-space. The material properties are given in Table 3, and it is noted that the clay is slightly softer than the sand considered in Case 1. Combined with the deeper top layer, this provides a lower cut-on frequency, around 7 Hz, compared to the cut-on frequency of 12.5 Hz in Case 1.

The resonance frequencies of the blocks within the WIB arrays can be found in Table 4. Notably, the resonance frequencies associated with the heave and pitch modes are higher than those in Case 1 (cf. Table 2), whereas the resonance frequencies related to sliding are lower. This can be explained by the soil deformation involved in the different modes of vibration. For the heave and pitch modes, the vertical motion of the SSI interfaces is important. Here, the impedance depends on the compressibility of the soil, which is low due to the high Poisson's ratio (0.4942) corresponding to nearly incompressible behaviour) compared to the Poisson's ratio in Case 1 (0.3330). On the other hand, the sliding mode is mainly influence by the shear stiffness, and since the shear modulus in Case 2 is about 10% lower than that in Case 1, the resonance frequency for the sliding mode can be expected to be lower as well.

Figure 6 shows the mean and quantile values of RL_3^2 and IL_3^{2j} (load placed at $y_{3\,2} = -2$ m) for Cases 2.1, 2.2, and 2.3, i.e. with block heights of 1 m, 2 m and 3 m, respectively, in Ring 1. Example results for the local variations within Case 2.3 are shown in Figure 7. Similarly, results for the load placed 8 m below the ground ($y_{3\,8} = -8$ m) are shown in Figure 8 and Figure 9.

For the load acting within the soft clay layer, 2 m below the ground surface, the reference vibration level within the receiver zone is small (about –45 dB) for frequencies below the cut-on frequency. A rapid increase in the RL can be seen from 7 Hz and up to about 14 Hz, where the TL has its maximum, around 7–8 dB. Beyond this peak, an almost linear monotonous decrease can be observed, reaching approximately –20 dB at 80 Hz.

The WIB arrays generally provide positive insertion loss when the load is placed at a depth of 2 m. With a block height of 1 m in Ring 1, the array delivers up to about 5–10 dB reduction in the vibration level within the receiver zone for the considered frequency range above 25 Hz. The effect of the second ring begins at around 30 Hz, and the third ring contributes to a further increase of the mean IL for frequencies above 35 Hz. The 2 m high blocks produce a mean IL comparable to that of the 1 m high blocks in most of the considered frequency range. As expected, a slight shift in the mean IL peaks towards lower frequencies can be seen. When the block height is further increase to 3 m, a significantly larger mean IL is obtained in the frequency range 18–25 Hz. The peak in the mean IL reaches 15 dB, independently of the number of rings in the array. However, the peak is slightly wider when two or three rings are present,

Soil layer (from top)	Shear modulus G [MPa]	Poisson's ratio ν [-]	Mass density ρ [kg/m^3]	Loss factor η [%]	Thickness h [m]
Clay, *soft, wet*	30.03	0.4942	1 694	4.50	5.0
Lime (half-space)	4 300	0.3500	2 100	2.00	∞

Table 3: Soil properties for Case 2.

	Blocks in Ring 1			Blocks in Ring 2			Blocks in Ring 3		
	Heave	Sliding	Pitch	Heave	Sliding	Pitch	Heave	Sliding	Pitch
Case 2.1	36.0	29.0	25.7	44.0	35.6	33.2	54.7	44.5	39.2
Case 2.2	25.4	20.5	9.85	31.1	25.2	12.9	38.7	31.4	15.0
Case 2.3	20.8	16.8	5.45	25.4	20.6	7.17	31.6	25.7	8.31

Table 4: Resonance frequencies (in Hz) of the blocks in Case 2.

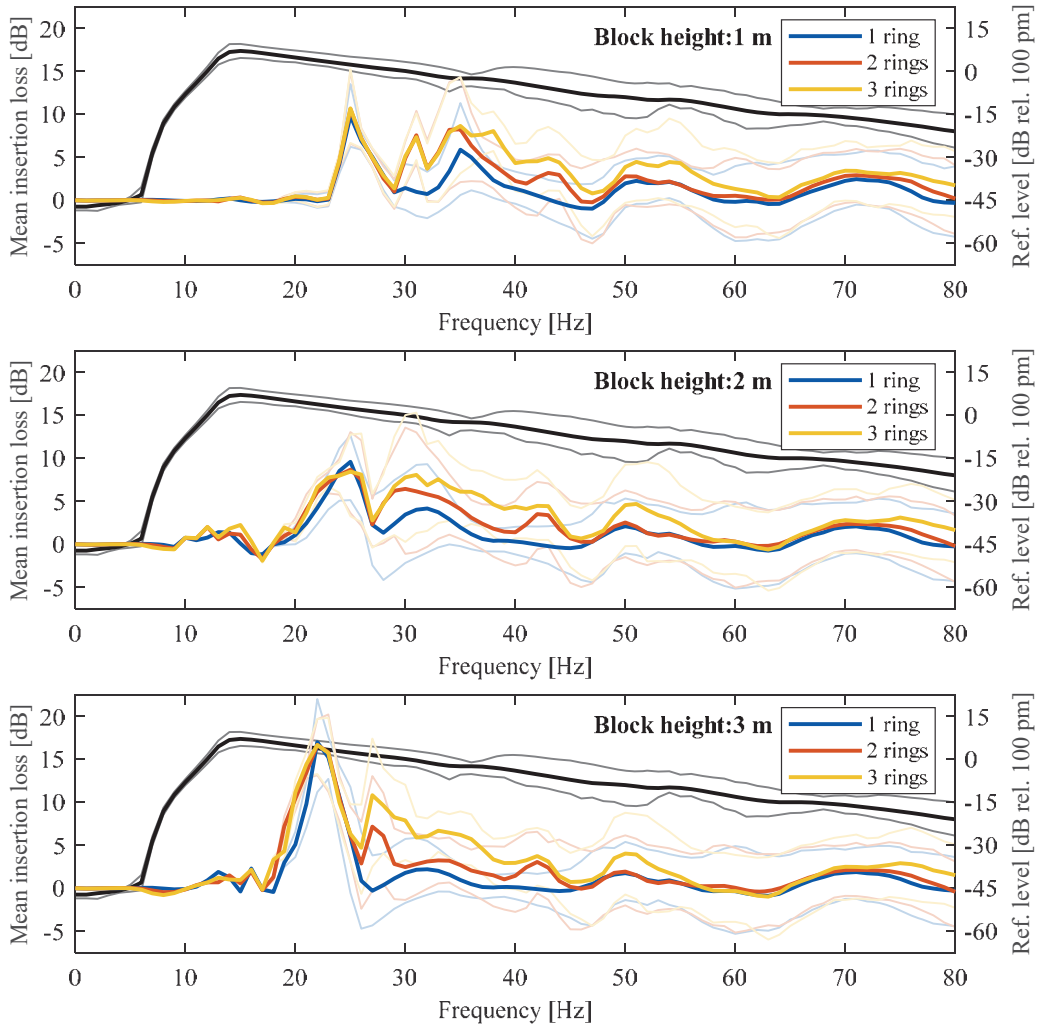

Figure 6: Mean ILs for the ground vibration within the donut-shaped surface area placed 20–40 m away from the centre of the load: Cases 2.1, 2.2, and 2.3 with the load acting 2 m below the ground. The black line shows the reference level of vibrations and the thin lines show the 10% and 90% quantiles of the respective quantities.

compared to the case with only one ring. For frequencies beyond 25 Hz, the ILs for Cases 2.1–2.3 are similar. Like it was found for Case 1, it can be observed that the WIB arrays have an effect in the frequency range where the WIBs may resonate.

The variations of the RL and IL produced by the 3 m high blocks (Case 2.3) are shown in Figure 7. Again, it is clearly seen that the effect of the WIB array is limited at low frequencies. The large IL observed around 18–25 Hz is also visible in this figure. However, even if the mean IL was previously found to reach nearly the same magnitude (15 dB), the subplots for the frequencies 20 and 25 Hz in Figure 7 show that the mean IL is the result of very different distributions for the array with only one ring versus the arrays with two or three rings. Especially, at 20 Hz the IL field is much more homogeneous and generally higher with two or three rings. This explains why the mean IL peak in Figure 6 is narrower for the array with one ring, and it also explains why the 10% and 90% quantile values are lower and higher, respectively, for one ring compared to two or three rings. Finally, at 30 Hz, zones with negative IL appear. A similar observation can be made for Case 1, with reference to Figure 3, where zones with negative IL

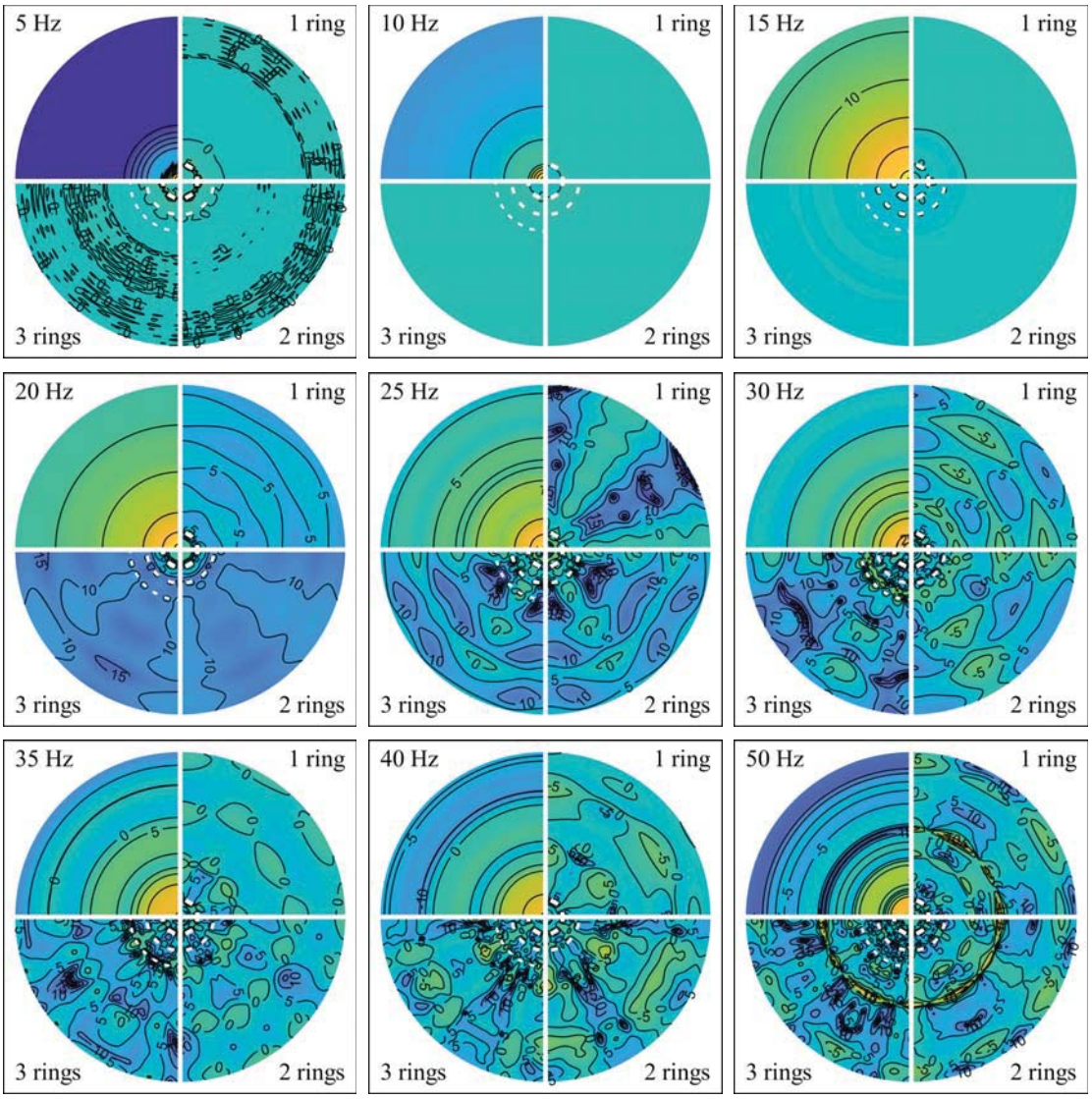

Figure 7: Contours of the reference vibration levels and ILs (in dB) for Case 2.3 with 1, 2, or 3 rings. The centre blocks are 3 m high and the vertical load is applied 2 m below the ground surface. Pale yellow/dark blue shades represent unfavourable/favourable values, respectively.

appear at 50 Hz. However, the mean IL is still positive at e.g. 50 Hz for both cases, when the load is applied 2 m below the ground surface (see Figures 2 and 4). For some higher frequencies, especially around 65 Hz in Case 1, a slightly negative mean IL is obtained. This should be seen in the context of the RL which is about 15–20 dB lower here compared to the maximum that occurs at around 20 Hz and 14 Hz in Cases 1 and 2, respectively. Further, the load spectra associated with pile driving can be expected to have less energy at higher frequencies.

Figure 8 shows the mean and quantile values of the RL and ILs in the receiver zone within Case 2, when the load is applied at 8 m depth. The RL is consistently below –35 dB rel. 100 pm in the entire frequency range relevant to whole-body vibration, i.e. up to 80 Hz. This is different when compared to Case 1, where an RL up to about –10 dB was obtained for frequencies slightly higher than the cut-on frequency of 12.5 Hz. A small local peak is also present in Case 2 for frequencies just above the cut-on frequency which is here around 7 Hz. However, this peak

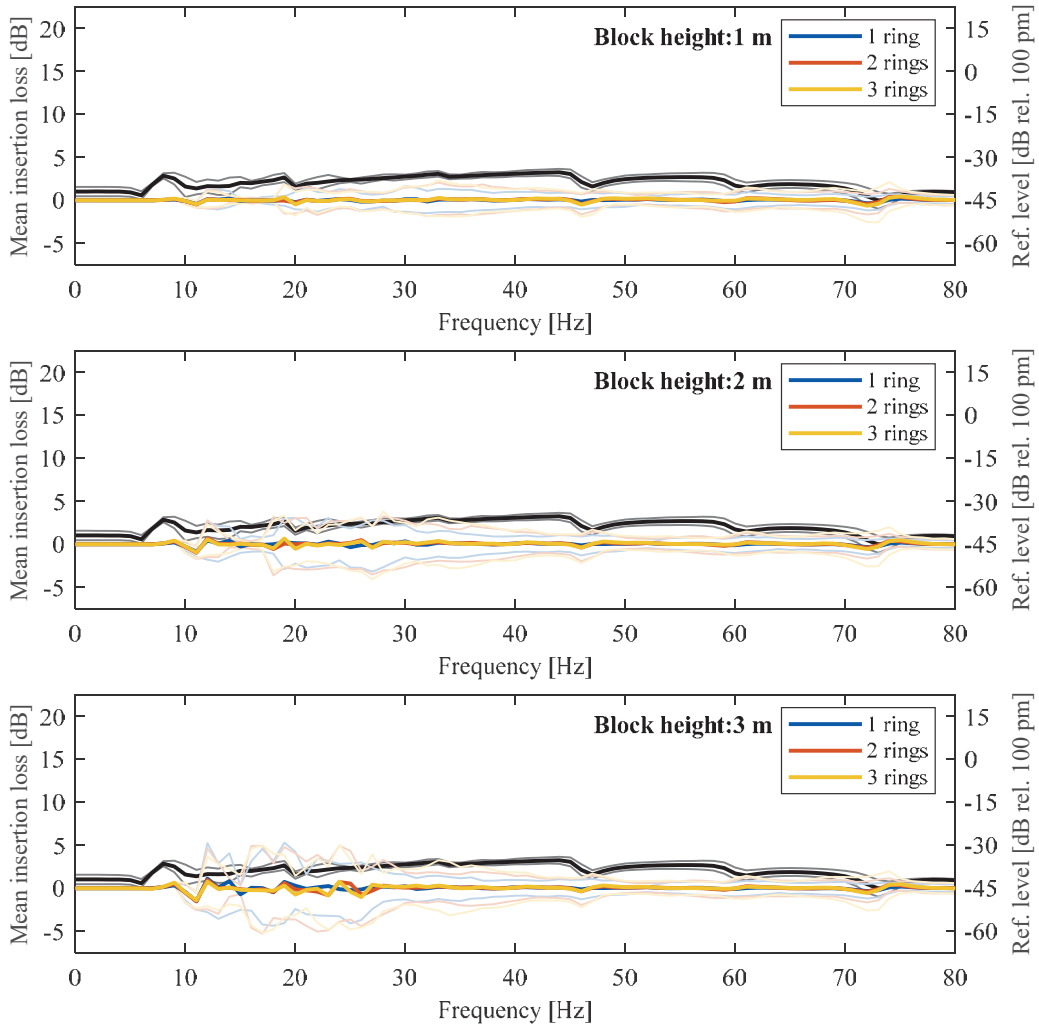

Figure 8: Mean ILs for the ground vibration within the donut-shaped surface area placed 20–40 m away from the centre of the load: Cases 2.1, 2.2, and 2.3 with the load acting 8 m below the ground. The black line shows the reference level of vibrations and the thin lines show the 10% and 90% quantiles of the respective quantities.

is much less pronounced, indicating that only a very small amount of the energy travelling within the ground enters the topsoil layer when the load is applied withing the lime half-space. This can be explained by the large impedance mismatch between the soft clay and the lime.

Compared to Case 1, more specifically by comparing Figures 4 and 8, it can be observed that the mean IL in Case 2 is nearly zero when the load is applied within the lime half-space, whereas some variation occurred in Case 1, when the load was applied within the till half-space. The very low impact of the WIB arrays on the IL can also be seen in Figure 9 which further shows that the number of rings has very limited influence. In Case 2 it is therefore even more pronounced, compared to Case 1, that the critical scenario will be related to loads applied within the soft topsoil. When the load acts within the deeper and stiffer soil, the transfer mobility to the ground surface is low.

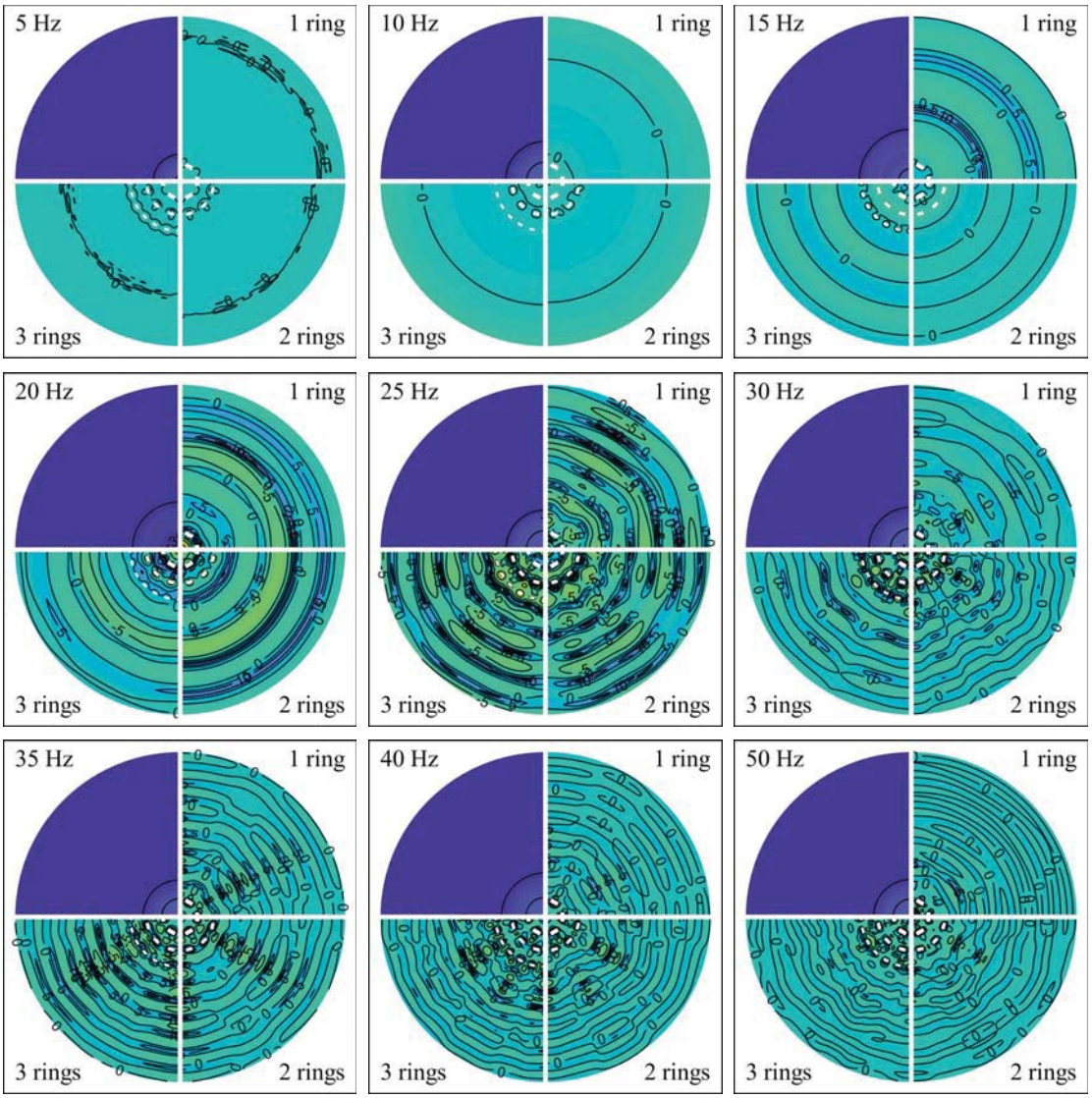

Figure 9: Contours of the reference vibration levels and ILs (in dB) for Case 2.3 with 1, 2, or 3 rings. The centre blocks are 3 m high and the vertical load is applied 8 m below the ground surface.
Pale yellow/dark blue shades represent unfavourable/favourable values, respectively.

5 CONCLUSIONS AND SUGGESTIONS FOR FURTHER RESEARCH

Based on a semi-analytical model of a layered soil, the insertion loss provided by circular arrays of monolithic blocks placed on the ground surface has been studied. It has been found that blocks placed in a so-called “Stonehenge” configuration effectively reduce the ground vibration level in a receiver zone 20–40 m away from the position at which a pile is driven into the soil. For two different cases, both of which consider a soft topsoil underlain by a stiffer half-space, an insertion loss of about 5–20 dB can be obtained by using blocks that could, on a construction site, be made from appropriate containers infilled with excavated soil or some heavy construction waste material. Adding more rings of wave impedance blocks to the array

will in most cases increase the insertion loss, but with an optimal tuning of the resonance frequencies, a significant reduction in the vibration level in the receiver zone can be achieved, even with a single ring of blocks, demonstrating the large mitigation potential of the solution.

In the present analyses, the pile has not been modelled explicitly. Instead, loads have been applied at different depths, in the soft topsoil or in the stiff half-space. When a pile is driven, forces will be transferred to the surrounding soil simultaneously along the shaft and the at the tip. Depending on the relative strengths of the soil down along the pile, the excitations produced along the shaft or at the tip may dominated. However, this cannot be modelled correctly by a simple viscoelastic model. Further research on the energy transfer mechanism between the pile and the soil is proposed in order to achieve more detailed quantification of the overall mitigation potential of circular block arrays.

Further, based on the observation that the block arrays are effective within the frequency range where the blocks may resonate, an optimization of the individual blocks is proposed for a future study. This can be combined with the optimization of the full array, focussed on placing the blocks on the ground such that the interference pattern of the scattered waves leads to an overall minimization of the transfer mobility within a selected receiver zone and for a given range of frequency.

Despite the shortcomings of the computational model, and knowing that a further potential for optimization exists, this study shows promise for an innovative technique where mitigation is placed *on* the ground surface which inhibits the transmission of vibration from *within* the body of the ground. Within the context of ground vibration, the method established here could be expected to apply to other scenarios with different source characteristics, i.e. different pile-driving methods. Developed further there could also be potential to study various source-types such as blasting or shock-vibration.

ACKNOWLEDGMENTS

The second author gratefully acknowledges the financial support from the Swedish Governmental Agency for Innovation Systems (Vinnova), grant ref. no. 2018-04159.

REFERENCES

[1] T. Münzel, F.P. Schmidt, S. Steven, J. Herzog, A. Daiber, M. Sørensen, Environmental Noise and the Cardiovascular System, J. Am. Coll. Cardiol. (2018). https://doi.org/10.1016/j.jacc.2017.12.015.

[2] T. Münzel, T. Gori, W. Babisch, M. Basner, Cardiovascular effects of environmental noise exposure, Eur. Heart J. (2014). https://doi.org/10.1093/eurheartj/ehu030.

[3] L. Andersen, S.R.K. Nielsen, Reduction of ground vibration by means of barriers or soil improvement along a railway track, Soil Dyn. Earthq. Eng. 25 (2005) 701–716.

[4] D.J. Thompson, J. Jiang, M.G.R. Toward, M.F.M. Hussein, E. Ntotsios, A. Dijckmans, P. Coulier, G. Lombaert, G. Degrande, Reducing railway-induced ground-borne vibration by using open trenches and soft-filled barriers, Soil Dyn. Earthq. Eng. 88 (2016) 45–59. https://doi.org/10.1016/j.soildyn.2016.05.009.

[5] A. Dijckmans, P. Coulier, J. Jiang, M.G.R. Toward, D.J. Thompson, G. Degrande, G. Lombaert, Mitigation of railway induced ground vibration by heavy masses next to the

track, Soil Dyn. Earthq. Eng. 75 (2015) 158–170. https://doi.org/10.1016/j.soildyn.2015.04.003.

[6] L. Andersen, A.H. Augustesen, Mitigation of traffic-induced ground vibration by inclined wave barriers – A three-dimensional numerical analysis, in: 16th Int. Congr. Sound Vib. 2009, ICSV 2009, 2009.

[7] L. Andersen, M. Liingaard, Vibration screening with sheet pile walls, in: H. Takemiya (Ed.), Environ. Vib. Predict. Monit. Mitig. Eval. (ISEV 2005), CRC Press, Taylor & Francis Group, London, Okayama, Japan, 20–22 September 2005, 2005: pp. 429–437.

[8] A. Dijckmans, A. Ekblad, A. Smekal, G. Degrande, G. Lombaert, Efficacy of a sheet pile wall as a wave barrier for railway induced ground vibration, Soil Dyn. Earthq. Eng. 84 (2016) 55–69. https://doi.org/10.1016/j.soildyn.2016.02.001.

[9] G.B. Warburton, J.D. Richardson, J.J. Webster, Forced Vibrations of Two Masses on an Elastic Half Space, J. Appl. Mech. 38 (1971) 148–156. https://doi.org/10.1115/1.3408735.

[10] G.B. Warburton, H.D. Richardson, J.J. Webster, Harmonic response of masses on an elastic half-space, J. Eng. Ind. Trans. ASME. 75 (1972) 158–170.

[11] A.T. Peplow, C.J.C. Jones, M. Petyt, Surface vibration propagation over a layered elastic half-space with an inclusion, Appl. Acoust. (1999). https://doi.org/10.1016/S0003-682X(98)00031-0.

[12] H. Masoumi, A. Van Leuven, S. Urbaniak, Mitigation of train induced vibrations by wave impeding blocks : numerical prediction and experimental validation, in: EURODYN 2014, 2014: pp. 863–870.

[13] D.J. Mead, Free wave propagation in periodically supported, infinite beams, J. Sound Vib. 11 (1970) 181–197. https://doi.org/10.1016/S0022-460X(70)80062-1.

[14] P. Persson, K. Persson, G. Sandberg, Reduction in ground vibrations by using shaped landscapes, Soil Dyn. Earthq. Eng. 60 (2014) 31–43.

[15] L.V. Andersen, Using periodicity to mitigate ground vibration, in: COMPDYN 2015 – 5th ECCOMAS Themat. Conf. Comput. Methods Struct. Dyn. Earthq. Eng., 2015.

[16] L.V. Andersen, P. Bucinskas, P. Persson, M. Muresan, L.-I. Muresan, I.-O. Paven, Mitigating ground vibration by periodic inclusions and surface structures, in: Proc. INTER-NOISE 2016 - 45th Int. Congr. Expo. Noise Control Eng. Towar. a Quieter Futur., 2016: pp. 7469–7480.

[17] L. V. Andersen, A. Peplow, P. Bucinskas, P. Persson, K. Persson, Variation in models for simple dynamic structure-soil-structure interaction problems, in: Procedia Eng., 2017: pp. 2306–2311.

[18] L.V. Andersen, A. Peplow, P. Bucinskas, Efficiency of nearly periodic structures for mitigation of ground vibration, in: 2017. https://doi.org/10.7712/120117.5439.18112.

[19] A. Peplow, L. Andersen, P. Bucinskas, Variations within simple models for structure-soil interaction, in: 24th Int. Congr. Sound Vib. ICSV 2017, 2017.

[20] A.T. Peplow, L.V. Andersen, P. Bucinskas, Environmental vibration reduction utilizing an array of mass scatterers, in: Procedia Eng., 2017. https://doi.org/10.1016/j.proeng.2017.09.359.

[21] G.A. Athanasopoulos, P.C. Pelekis, Ground vibrations from sheetpile driving in urban environment: Measurements, analysis and effects on buildings and occupants, Soil Dyn. Earthq. Eng. 19 (2000) 371–387. https://doi.org/10.1016/S0267-7261(00)00008-7.

[22] F. Deckner, K. Viking, S. Hintze, Aspects of ground vibrations due to pile and sheet pile driving, Electron. J. Geotech. Eng. 20 (2015) 11161–11176.

[23] F. Deckner, K. Viking, C. Guillemet, S. Hintze, Instrumentation system for ground vibration analysis during sheet pile driving, Geotech. Test. J. 38 (2015) 893–905. https://doi.org/10.1520/GTJ20140275.

[24] F. Deckner, K. Viking, S. Hintze, Wave Patterns in the Ground: Case Studies Related to Vibratory Sheet Pile Driving, Geotech. Geol. Eng. 35 (2017) 2863–2878. https://doi.org/10.1007/s10706-017-0285-x.

[25] L. V Andersen, A.T. Peplow, P. Persson, Mitigation of ground vibrations by circular arrays of rigid blocks, in: M. Papadrakakis, M. Fragiadakis (Eds.), Proc. 7th Int. Conf. Comput. Methods Struct. Dyn. Earthq. Eng. Vol. 2, National Technical University of Athens, Athens, 2019: pp. 3422–3447.

[26] A.F. Homayoun Rooz, A. Hamidi, A numerical model for continuous impact pile driving using ALE adaptive mesh method, Soil Dyn. Earthq. Eng. 118 (2019) 134–143. https://doi.org/10.1016/j.soildyn.2018.12.014.

[27] W.T. Thomson, Transmission of elastic waves through a stratified solid medium, J. Appl. Phys. 21 (1950) 89–93.

[28] N.A. Haskell, The dispersion of surface waves on multilayered media, Bull. Seismol. Soc. Am. 43 (1953) 17–34.

[29] L. Andersen, J. Clausen, Impedance of surface footings on layered ground, Comput. Struct. 86 (2008) 72–87.

[30] R. Wang, A simple orthonormalization method for stable and efficient computation of Green's functions, Bull. Seismol. Soc. Am. 89 (1999) 733–741.